Earthquakes and Structures, *Vol. 18, No. 4 (2020) 423-435*
DOI: https://doi.org/10.12989/eas.2020.18.4.423

Assessment of seismic damage on frame structures across the earth fissure under earthquake

Zhongming Xiong[1,2,3a], Xiaopeng Huo[1,2,3b], Xuan Chen*[1,2,3], Jianjian Xu[1,2,3c], Weiyang Xiong[4d] and Yan Zhuge[5e]

[1]*School of Civil Engineering, Xi'an University of Architecture & Technology, Xi'an 710055, China*
[2]*Key Lab of Structural Engineering and Earthquake Resistance, Ministry of Education (XAUAT), Xi'an 710055, China*
[3]*Shaanxi Key Lab of Structure and Earthquake Resistance(XAUAT), Xi'an 710055, China*
[4]*Graduate School of Arts and Science, New York University, New York 10003, U.S.A.*
[5]*School of Natural & Built Environments, University of South Australia, Adelaide 5095, Australia*

(*Received April 26, 2019, Revised August 21, 2019, Accepted November 26, 2019*)

Abstract. An accurate evaluation of structural damage is essential to performance-based seismic design for the structure across the earth fissure. By comparing the calculation results from three commonly used damage models and the experimental results, a weighted combination method using Chen model was selected in this paper as the seismic damage evaluation. A numerical model considering the soil-structure interaction (SSI) was proposed using ABAQUS software. The model was calibrated by comparing with the experimental results. The results from the analysis indicated that, for the structure across the earth fissure, the existence of earth fissure changed the damage distribution of the structural members. The damage of structural members in the hanging wall was greater than that in the foot wall. Besides, the earth fissure enlarged the damage degree of the structural members at the same location and changed the position of the weak story. Moreover, the damage degree of the structure across the earth fissure was greater than that of the structure without the earth fissure under the same excitation. It is expected that the results from this research would enhance the understanding of the performance-based seismic design for the structure across the earth fissure.

Keywords: earth fissure; frame structure; damage model; performance-based seismic design; soil-structure interaction

1. Introduction

Earth fissures, occurred in many countries around the world, have become a serious geological hazard ((Ayalew *et al*. 2004, Jachens and Holzer 1982, Wartman *et al*. 2003, Yu *et al*. 2010). They would cause the destruction of building structures, road cracks and pipeline ruptures, which have a great impact on the construction of urban projects and the daily life of residents. Studies on the formation of earth fissures have been widely reported since they were first discovered in the United States. It is commonly accepted that earth fissures were usually caused by the tectonic activities and the ground water extraction ((Budhu and Adiyaman 2012, Li *et al*. 2006, Peng *et al*. 2016, Rajendran *et al*. 2003, Sancio *et al*. 2002).

In general, avoidance measures had been adopted to reduce the harm of earth fissure to engineering structures. With the development of existing earth fissures and the appearance of new earth fissures, many structures which were not affected by earth fissures in the past, have become vulnerable to the earth fissure damage. The influence of earth fissure on structure was studied by many researchers (Liu 2015, Wang *et al*. 2016, Xiong *et al*. 2018). Peng *et al*. (2012) proposed that the damage degree of the underground structure was related to the development of earth fissures. Liu *et al*. (2017) proposed using flexible joints to reduce the influence of earth fissure on a metro tunnel under earthquake. Xiong *et al*. (2018) conducted a shaking table test to analyze the seismic performance of a RC frame across the earth fissure, and analyzed the influence of earth fissures on the dynamic response. To date, many studies have been carried out on the dynamic response of earth fissure to surface structures or underground structures. However, based on the authors' knowledge, there is no study on seismic damage for structures on the earth fissure site (Xiong *et al*. 2019).

The assessment of seismic damage of structures is to determine whether the structure under earthquake could meet the requirements for seismic resistance. The seismic damage would also affect the structural function and safety. Therefore, it is necessary to estimate the seismic damage of structure across the earth fissure.

In recent decades, performance-based design (Ghobarah *et al*. 2015, Kostinakis and Morfidis 2017) has been widely adopted for the assessment of seismic damage. There are two major methods have been adopted: the integral method and the weighted combination method. In the integral

*Corresponding author, Ph. D. Student
E-mail: chenxuan@xauat.edu.cn
[a]Professor
[b]Ph.D. Student
[c]Master Student
[d]Master Student
[e]Professor

http://www.techno-press.org/?journal=eas&subpage=7 ISSN: 2092-7614 (Print), 2092-7622 (Online)

method, the structure is analyzed as a whole, and the effect of local component damage on the whole structure is neglected. In the combination method, the effect of local component damage is considered and earthquake damages in member-level, story-level and structure-level needs to be assessed. The analysis steps of the weighted combination method are as follows: firstly, the damage index of each story is obtained by analyzing the damage of each story in the structure; secondly, the damage index of the whole structure is obtained by weighting combination according to weight coefficients. In general, the weighted combination method needs some assessment of earthquake damage in member-level, story-level and structure-level. Many damage models for different levels have been proposed by many researchers, and most of them are commonly based on normalized deformation, hysteretic energy or a combination of both (Ayalew *et al.* 2004, Dong *et al.* 2018, Ghobarah *et al.* 2015, Ghosh and Collins 2010, Li *et al.* 2017). Among them, a damage model with the combination of deformation and hysteretic energy has been proved as a better indicator of seismic damage of structures.

The work carried out herein aims to estimate the damage degree for the frame structure across the earth fissure under the earthquake. A proper method to evaluate the damage will be proposed through analysis and comparison of shaking table test results. The effect of earth fissure on the seismic structural damage will be discussed and evaluated through numerical analysis.

2. Damage indices

2.1 Damage indices in member-levels

Generally, seismic damage of a structure is accumulating under a moderately strong to a very strong earthquake, it needs a proper assessment of the damage in structural members. In the performance-based seismic design method, 'damage index' was proposed to evaluate the seismic damage in a structure under the earthquake. In most cases, damage indices are dimensionless parameters intended to range between 0 (for an undamaged structure) to 1 (for a fully damaged or collapsed structure), with intermediate values giving some measure of the degree of partial damage. The most widely explored damage indices were based on displacement and energy. Park and Ang (1985) proposed a damage index for reinforced concrete structures in member-levels and story-levels, which consisted of normalized deformation and hysteric energy absorption, as shown in Eq. (1).

$$D = \frac{x_m}{x_{cu}} + \beta \frac{E_h}{F_y x_{cu}} \tag{1}$$

where x_m is the maximum deformation under earthquake; x_{cu} is the ultimate deformation under monotonic loading; β is the energy dissipation factor; E_h is the absorbed hysteretic energy; and F_y is the yield strength.

Niu and Ren (1996) defined a damage index with a nonlinear combination of the maximum deformation and hysteric energy absorption, which was based on the actual earthquake damage in RC frame structures and the statistical analysis of the data. The damage index iin Eq. (2)

$$D = \frac{x_m}{x_{cu}} + \alpha(\frac{E_h}{E_u})^{\beta} \tag{2}$$

where Eu is ultimate hysteretic energy; α and β are the combination factors; the definition of other parameters are the same as in Eq. (1).

Later on, Chen *et al.* (2010) proposed a modified damage model to solve the issue of convergence on the boundary of the Park-Ang damage model, as follows

$$D = \frac{x_m}{x_{cu}} + \alpha(\frac{E_h}{E_u})^{\beta} \tag{3}$$

where X_y is the yield deformation of a member; the meanings of the other parameters are same as in Eq. (1). (1-β) and β in the improved model were used to describe the ratio of deformation and energy to structural damage, so that the damage index is not more than 1.

To find out the most suitable damage assessment method for the structural members across the earth fissure, all three models discussed above will be used to evaluate the seismic damage in story-levels of structures across the earth fissure and the results will be compared.

2.2 Damage indices in structure-levels

There are two kinds of methods which could assess the structure damage, known as the global methods and the weighted combination methods. Global methods are to get the damage index by analyzing the response characteristics of the whole structure under the earthquake, such as the attenuation of the vibration frequency of the structure and the degeneration of the stiffness; weighted combination methods are to get the damage index of the whole structure by weighting the damage index of the structural members as mentioned above.

2.2.1 Global methods

To evaluate the structural damage, a global model with considering the change in the fundamental period of the structure before and after the earthquake was proposed by DiPasquale and Cakmak (1987)

$$D = 1 - \frac{f_i^2}{f_0^2} \tag{4}$$

where f_i is the fundamental period of the structure after the earthquake; f_0 is the fundamental period of the structure before the earthquake.

Ghobarah *et al.* (2015) adopted the static elastoplastic method and proposed a global damage model which is based on the stiffness degradation of structures before and

Table 1 Damage state corresponding to different damage index

State description	Value for global damage value D			
	Park-Ang	Ghobarah	Niu (Ou)	Chen (Ou)
No damage or small local cracks	D<0.1	D<0.15	D<0.2	D<0.2
Slight damage, small cracks	0.1 ≤ D< 0.25		0.2≤D<0.4	0.2≤D<0.4
Medium damage	0.25≤D<0.4	0.15≤D<0.3	0.4≤D<0.65	0.4≤D<0.6
Severe damage	0.4≤D<1	0.3≤D<0.8	0.65≤D<0.9	0.6≤D<0.9
Collapse	D≥1	D≥0.8	D≥0.9	D≥0.9

after earthquakes

$$D = 1 - \frac{K_{final}}{K_{initial}} \tag{5}$$

where K_{final} is the stiffness of the structure after the earthquake; $K_{initial}$ is the stiffness of the structure before the earthquake.

2.2.2 Weighted combination methods

Based on the damage in member-levels proposed by Park and Ang (1985) a structural damage model is defined as

$$D = \sum_i w_i D_i \tag{6}$$

$$w_i = \frac{E_i}{\sum E_i} \tag{7}$$

where D_j is the damage index of member j; where w_i is the weight coefficient which means the proportion of energy consumption of members in the total energy consumption of the structure.

Wu and Ou (1993) improved the Park-Ang damage model by considering the effects of weak story and number of stories on structural damage, as shown in Eq. (8) and Eq. (9).

$$D = \sum_{j=1}^{n} w_j D_j \tag{8}$$

$$w_j = \frac{(n+1-j)D_j}{\sum_{j=1}^{n}(n+1-j)D_j} \tag{9}$$

where D_j is the damage index of story j; w_j is the weight coefficient of story j; n is the number of storys in the structure; according to this theory, the lower the story is, the greater the proportion of members in the overall structural damage. Among them, the damage indices of stories could also be calculated by Eq. (1) - (3). In this formulas, the x_m is the maximum story drift under earthquake; x_{cu} is the minimum limit displacement of columns under monotonic loading; E_h is the energy dissipation of all the members at a story; β is the energy dissipation factor for a story; and F_y is the yield shear force of a story.

RC structures usually allow a certain degree of damage.

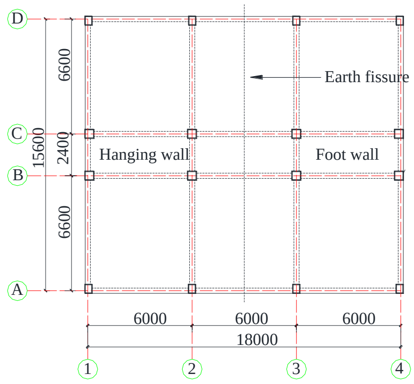

(a) Plane layout

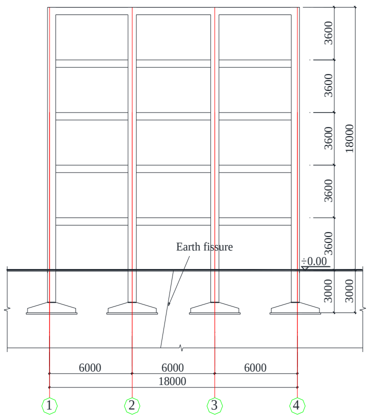

(b) Elevation layout

Fig. 1 Configurations of the prototype structure (unit: mm)

It is therefore important to precisely determine the damage state for a structure; definitions on damage index to damage states for global structure were proposed in their studies, which are shown in Table 1 (Chen *et al*. 2010, Ghosh and Collins 2010, Niu and Ren 1996, Ou *et al*. 1999, Park and Ang 1985).

3. Development of the damage index of structures across the earth fissure

3.1 Experimental testing program

The test model considered in the studies is a five-story RC frame structure across the earth fissure in Xi’an, China (Xiong *et al*. 2018). The dimension of the prototype

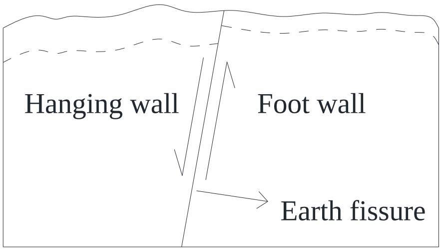

Fig. 2 The deformation of the earth fissure under tectonic action

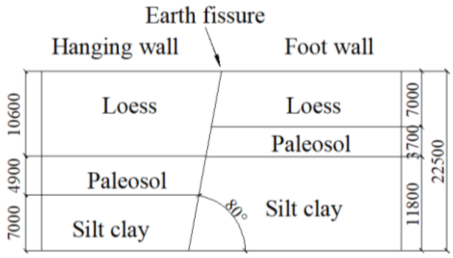

(a) The site with the earth fissure

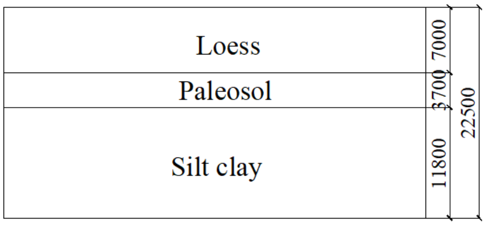

(b) The site without the earth fissure

Fig. 3 Configurations of soil sites (unit: mm)

structure is 18 m ×15.6 m and the height of each story is 3.6 m. The structure is regular in plane, with uniform distribution of stiffness and mass. The layout of the structure is shown in Fig. 1

Fig. 2 shows the deformation of the earth fissure under tectonic action. The earth fissure divided the soil site into hanging wall and foot wall. The hanging wall was above the earth fissure, and the foot wall was below the earth fissure. Under the tectonic action, vertical settlement would occurred in the earth fissure. And the settlement of the hanging wall is always greater than that of foot wall, forming the uneven settlement (Liu *et al*. 2017, Xiong *et al*. 2019).

This study is focused on the earth fissure under earthquake. Based on the geotechnical investigation report (Wei Cai Ping *et al*. 2013), the width of earth fissure was 0.1-5 mm, which are stable in static load. As shown in Fig. 3(a), the soil layer of the earth fissure zone is divided into three layers from top to bottom: loess layer, paleosol layer and silt clay layer. The soil was divided into hanging wall and foot wall with an inclination of 80° by the earth fissure. For comparison, a site without the earth fissure was also set up, as shown in Fig. 3(b). The material properties of the soil were shown in Table 2.

Based on the test conditions and structural characteristics, a scaled model was used and the scale ratio of the model is determined to be 1:15. The size of structure

Table 2 Material properties of the soil from the ground fissure area

Material	Unit weigh (kN/m3)	Moisture content (%)	Cohesion (kPa)	Internal friction angle (°)	Shear modulus (MPa)
Loess	16.8	23.5	48	27.6	110.49
Paleosol	17.8	22.9	49	27.3	139.45
Silty Clay	19.0	25.2	45	26.6	163.34

Table 3 Similitude scale factors

Physical quantity	Relationship	Value	
		Model structure	Model soil
Length	S_l	1/15	1/15
Elastic modulus	S_E	0.1677	2/15
Stress	S_σ	0.1677	–
Strain	S_σ / S_E	1	–
Equivalent density	$S_\rho = S_E/(S_l \cdot S_a)$	1.258	1
Mass	$S_m = S_\rho \cdot S_l^3$	5.592×10^{-4}	–
Duration	$S_t = \sqrt{s_l/s_a}$	0.183	0.183
Frequency	$S_\omega = 1/S_t$	5.47	5.47
Acceleration	S_a	2	2

Fig. 4 Test model

is 1200 mm × 1040 mm × 1400 mm. Based on the Buckingham π theorem, the similarity relationship among the physical quantities could be deduced, which shown in Table 3 (Krawinkler and Moncarz 1981).

Moreover, a laminar shear box was used as the model soil container. To reduce the boundary effect on vibration direction, and some rubber foam plastic plates were pasted on inner layer of the container. The test model is show in Fig. 4.

As shown in Fig. 5, the test model was set with 40 transducers to measure displacements and accelerations. To record the dynamic response of the model structure, the accelerometers and displacement meters were fixed at each story. To find the effect of the earth fissure on the dynamic response of model soil, the accelerations were measured with accelerometer arranged in the soil. And the input base acceleration could be measured by the accelerometer posted on the shaking table. Based on the data of the displacements and accelerations, the interlayer shear and the interlayer deformation of model structure could be calculated, which are necessary to establish the damage index.

In the test, Jiangyou, El Centro and Cape Mendocino

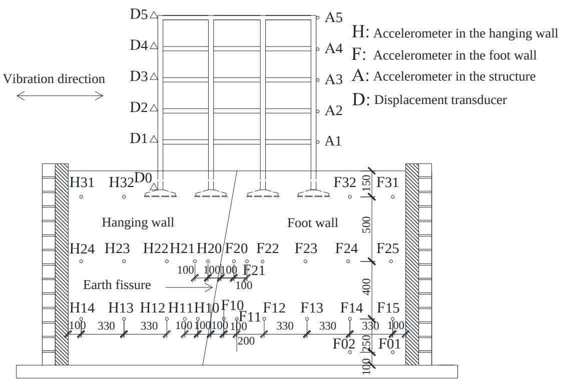

Fig. 5 The positions of the measuring transducers

Table 4 Test cases for the shaking table tests

Test sequence	Input	PGA (g)	
		Model structure	Prototype structure
1	White noise	0.050	0.025
2	Jiangyou record	0.100	0.050
3	El Centro record	0.100	0.050
4	Cape Mendocino record	0.100	0.050
5	White noise	0.050	0.025
6	Jiangyou record	0.200	0.100
7	El Centro record	0.200	0.100
8	Cape Mendocino record	0.200	0.100
9	White noise	0.050	0.025
10	Jiangyou record	0.300	0.150
11	El Centro record	0.300	0.150
12	Cape Mendocino record	0.300	0.150
13	White noise	0.050	0.025
14	Jiangyou record	0.400	0.200
15	El Centro record	0.400	0.200
16	Cape Mendocino record	0.400	0.200
17	White noise	0.050	0.025
18	Jiangyou record	0.600	0.300
19	El Centro record	0.600	0.300
20	Cape Mendocino record	0.600	0.300
21	White noise	0.050	0.025
22	Jiangyou record	0.800	0.400
23	El Centro record	0.800	0.400
24	Cape Mendocino record	0.800	0.400
25	White noise	0.050	0.025
26	Jiangyou record	1.200	0.600
27	El Centro record	1.200	0.600
28	Cape Mendocino record	1.200	0.600
29	White noise	0.050	0.025

seismic waves were selected as the input motions. The first two seismic waves were from the surface while the last seismic wave was from the bedrock. An earth record from the bedrock was added to consider the effect of high-frequency components of seismic waves on the dynamic response of the test model. To investigate the damage degree of the model structure in different intensities, these ground motions were scaled to seven levels (0.1, 0.2, 0.3, 0.4, 0.6, 0.8 and 1.2 g), which were input from the shanking table. Before and after each series of ground acceleration inputs, white noise tests were conducted to establish the natural frequencies of the structure. The test cases are shown in Table 4.

3.2 Test phenomena

Fig. 6 presents the local crack patterns after earthquake excitation. When the peak ground acceleration (PGA) of the input seismic wave reached 0.2 g (small earthquake), there was a slight concrete spalling occurred at the top of a column of the structure at the fourth story on the hanging wall (Fig. 6(a)). At the same time, some small vertical cracks occurred in a beam of the model on the fourth story (Fig. 6(b)). When the PGA reached 0.4 g (moderately strong earthquake), the structure shook obviously, and the existing cracks continued to expand along the cracking direction. Vertical cracks were observed at some beam column joints on the first and second story (Fig. 6(c)), and tiny cracks were found at the top of a column on the fifth story (Fig. 6(d)). When the PGA reached 0.8 g (strong earthquake), crack transfixion appeared at some beams and columns, resulting in the separation of beams and columns from plates (Fig. 6(e) - (f)).

During the test, cracks appeared earlier in the hanging wall area than those in the foot wall area and the cracks of members on the hanging wall developed acutely than those on the foot wall. In addition, the development of cracks was more obvious at the lower story. Overall, under the earthquake action, the frame structure across the earth fissure on the hanging wall suffered more serious damage than that on the foot wall, and the damage of the lower story was more serious than that of the higher stories.

3.3 Acceleration response of the model soil

Fig. 7 shows peak acceleration magnification factors of the model soil in the earth fissure areas, in which the acceleration meters are buried in the model soil. As shown in Fig. 7, the magnification factors of model soil at different measuring points were basically greater than 1. The amplification factors of measuring points were the largest at H12, which were closed to the earth fissure. Generally, the magnification factors in the hanging wall were obviously greater than these of the foot wall with same distance from the earth fissure. In addition, as the PGA of input waves increased, the peak acceleration magnification factors decreased, which was due to the softening and stiffness degradation of the model soil.

It is noted that the intensity of the seismic waves would increase after the propagation of the waves in the soil with the earth fissure, which was different from that in the unfissured site. And the levels of dynamic magnification were related to position of measuring points in the earth fissure site. The intensity of the waves were different in the hanging wall and foot wall, formatting the non-uniform excitation for the engineering structures in the earth fissure site.

3.4 Damage analysis on story-level

Park-Ang model, Niu model and Chen model were

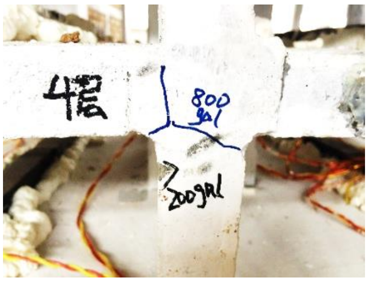

(a) Concrete spalling at the top of a column on the fourth story

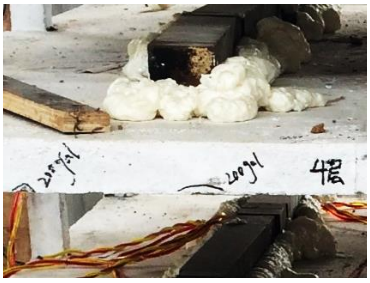

(b) Small cracks in the beam on the fourth story

(c) Cracks at a beam column joint on the second story

(d) Tiny cracks at the top of a column on the fifth story

(e) Beam-end cracks on the third story

(f) Cracks on the top story

Fig. 6 Damage on the model structure

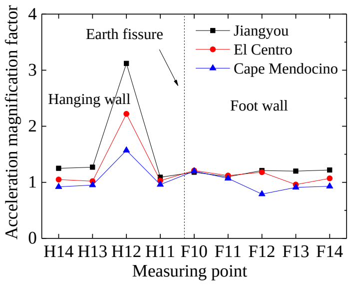

(a) 0.2 g

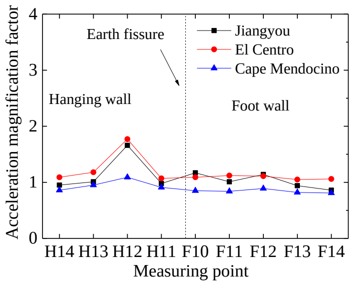

(b) 0.4 g

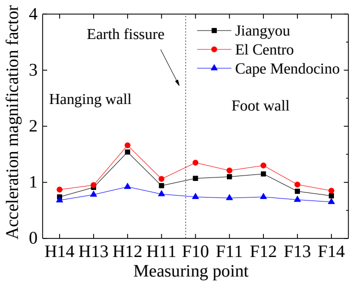

(c) 0.8 g

Fig. 7 Acceleration amplification factors of model soil under different waves

Table 5 Damage indices of local stories at different seismic waves

Seismic wave	Story	PGA=0.2 g			PGA=0.4 g			PGA=0.8 g		
		Park-Ang	Niu	Chen	Park-Ang	Niu	Chen	Park-Ang	Niu	Chen
Jiangyou record	5	0.141	0.243	0.129	0.340	0.451	0.320	0.650	0.755	0.624
	4	0.132	0.242	0.127	0.290	0.401	0.284	0.558	0.658	0.551
	3	0.174	0.284	0.164	0.407	0.515	0.397	0.637	0.736	0.626
	2	0.227	0.338	0.213	0.475	0.578	0.471	0.832	0.926	0.809
	1	0.247	0.359	0.235	0.513	0.613	0.510	1.011	1.100	0.982
El-Centro record	5	0.117	0.214	0.106	0.282	0.394	0.267	0.552	0.658	0.533
	4	0.106	0.214	0.100	0.270	0.381	0.265	0.478	0.581	0.474
	3	0.166	0.275	0.155	0.381	0.490	0.370	0.596	0.696	0.587
	2	0.194	0.304	0.183	0.432	0.540	0.422	0.807	0.903	0.786
	1	0.246	0.357	0.233	0.484	0.586	0.483	0.933	1.025	0.905
Cape Mendocino record	5	0.143	0.243	0.130	0.370	0.481	0.342	0.624	0.729	0.599
	4	0.133	0.237	0.122	0.322	0.434	0.307	0.560	0.664	0.546
	3	0.191	0.298	0.176	0.432	0.543	0.408	0.734	0.834	0.710
	2	0.248	0.354	0.227	0.517	0.627	0.492	0.870	0.967	0.839
	1	0.270	0.381	0.253	0.553	0.657	0.538	1.037	1.131	0.997

selected to evaluate the seismic damage of the structure at each story. Based on the basic information of structural members and formulas mentioned under Section 2, the damage indices of stories were calculated. It is noted that Eh in the experiment is based on the area of the interlayer displacement-interlayer shear curve. Table 5 shows the

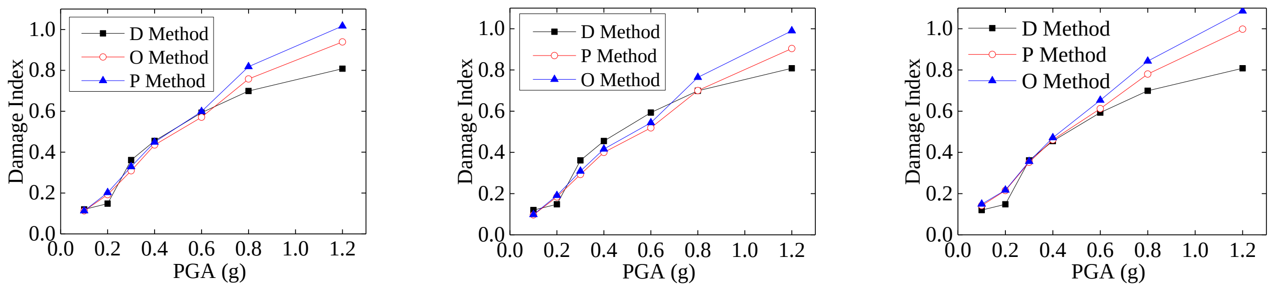

(a) Under Jiangyou wave (b) Under El Centro wave (c) Under Cape Mendocino wave

Fig. 8 The seismic damage index on the structure calculated by different methods

damage indices of local stories under different seismic waves.

As shown in Table 5, the damage index calculated by Niu model is the largest and Chen model is the smallest. In addition, there is very small difference of the results between Chen model and Park-Ang model. The damage index of the structure was the largest in the first story and smallest in the fourth story, which indicated that the frame structure across the earth fissure suffered serious damage at the first story under the earthquake.

According to the damage state corresponding to different damage indices in Table 1, the damage degree of the structure was evaluated under three damage models. As shown in the calculation results using Chen model, the structure at the first story suffered slightly damage, medium damage, severe damage under the seismic wave with the PGA of 0.2 g, 0.4 g and 0.8 g, which was consistent with the experimental results. However, the damage states of the model structure through calculation results using Niu and Park-Ang models were exaggerated comparing to the damage states observed from the experimental phenomena. Therefore, Chen model was selected to estimate the seismic damage on the structure across the earth fissure for the structure-level.

3.5 Damage analysis on structure-level

To find out an optimal method for evaluating the seismic damage on structure-level for the structure across the earth fissure, a global method and two weighted combination methods were adopted to compare the advantages and disadvantages of each method.

Fig. 8 depicts the structural damage index obtained by different methods. Among them, the natural frequency attenuation method was selected as a global model defined as Method D to evaluate the structural damage. The weighted combination method proposed by Park and Ang is defined as Method P, and the combination model proposed by Ou is defined as Method O.

When the natural frequency attenuation method is used to evaluate the damage degree of the whole structure, the damage index from the calculation would underestimate the damage degree of the structure when the PGA is small. The Method P would overestimate the damage degree of the structure when the PGA is large. Comparatively, the damage degree of the structure derived by the O Method was most close to the testing results. Therefore, the O Method was chosen to carry out the damage analysis on the structure across the earth fissure for the structure-level.

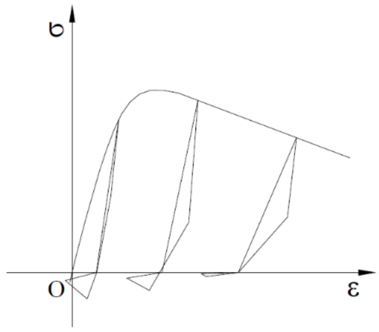

(a) Constitutive relation of concrete

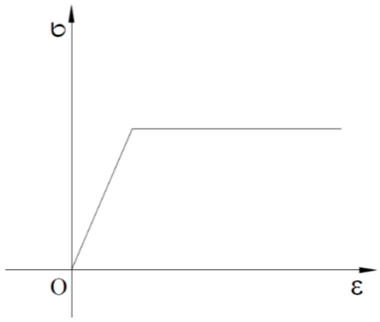

(b) Constitutive relation of rebar

Fig. 9 Constitutive model for concrete and rebar

4. Numerical simulation

4.1 Numerical modelling

In order to study the influence of earth fissure on seismic response of frame structure, the finite element model of the structure in earth fissure site and that in the site without earth fissure were established by using ABAQUS software, which is based on the size of the prototype structure.

For the purpose of this study, beam elements were used to simulate beams and columns of the model structure; shell elements were used to simulate slabs; solid elements were used to simulate the soil. Considering the tensile strength and damage degradation, UConcrete02 model was adopted as the constitutive model for concrete structures under

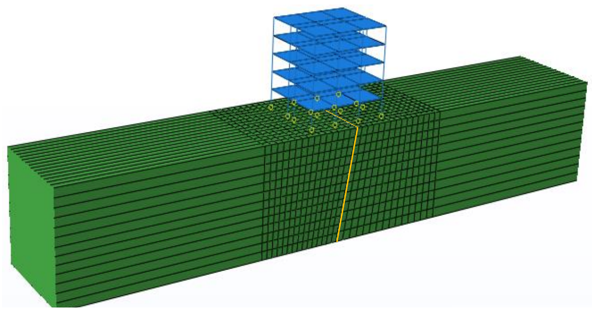

(a) The structure across the earth fissure

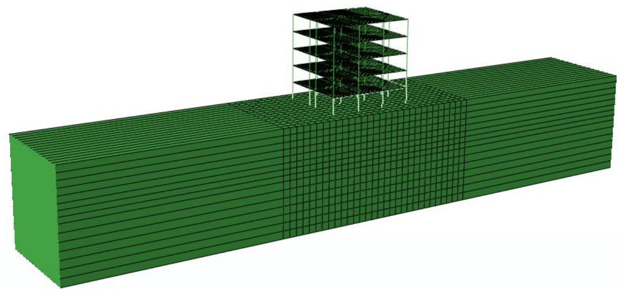

(b) The structure in the site without the earth fissure

Fig. 10 The finite element model

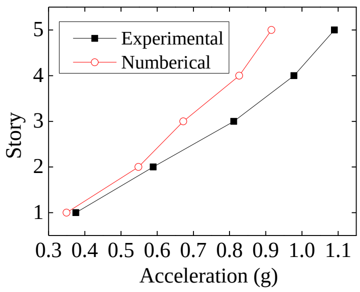

(a) Under Jiangyou wave with PGA of 0.2 g

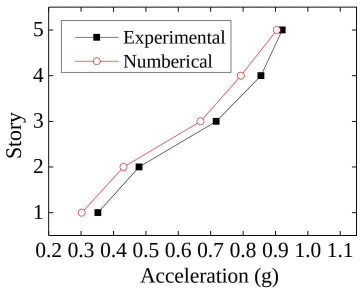

(b) Under El Centro wave with PGA of 0.2 g

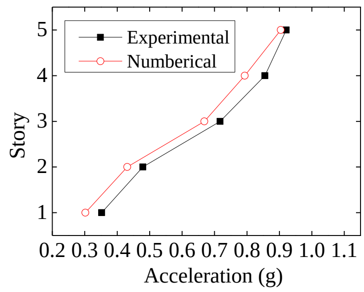

(c) Under Cape Mendocino wave PGA of 0.2 g

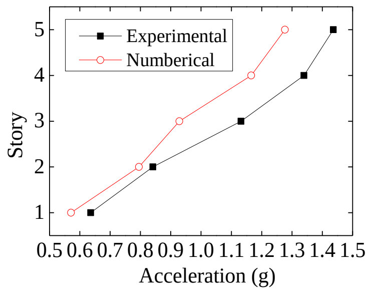

(d) Under Jiangyou wave with PGA of 0.4 g

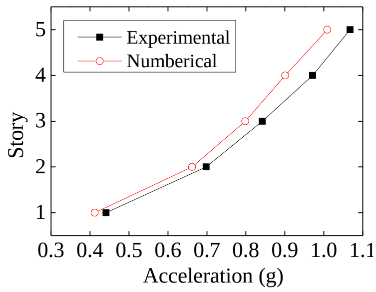

(e) Under El Centro wave with PGA of 0.4 g

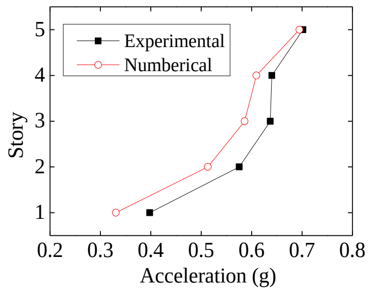

(f) Under Cape Mendocino wave PGA of 0.4 g

Fig. 11 Peak acceleration comparison of the structure across the earth fissure

earthquake. The perfectly elastoplastic model for rebar was used in this study (2009). Fig. 9 presents the constitutive model for concrete and rebar.

During the establishment of soil model for earth fissure site, the hanging wall and foot wall were respectively established. The soil profiles from earth fissure were defined laterally unseparated before earthquake loading in the simulation. And the hanging wall and football would contact or separate under earthquake. Earth fissure action was simulated by setting an appropriate contact surface between hanging wall and foot wall. The normal action was set to hard contact, and tangential action was simulated by setting penalty friction. After the model structure and the model soil were established, the finite element model considering the soil-structure-interaction was established by coupling the frame structure and the soil. Along the direction of the input seismic wave, boundaries with infinite element were set on both sides of the soil, which could solve the reflection and scattering effects of seismic waves at the boundaries (Zhao *et al*. 2013). Moreover, Rayleigh damping was adopted in this numerical simulation, and the damping ratio was set as 5 %. The finite element models are presented in Fig. 10. The distribution of soil layer in the site without earth fissure was consistent with the distribution of the soil layer in the footwall of the earth fissure site.

4.2 Comparison between numerical and experimental results

In order to verify the numerical model, the maximum acceleration of the structure across the earth fissure at each story in the numerical and experimental results was analyzed and compared under earthquake. It was noted that the experimental results were converted for the prototype structure according to the similarity relationship. Fig. 11 presents the peak accelerations of the model structure comparison between numerical results and experimental results.

As shown in Fig. 11, change trends of the maximum acceleration of the structure at each story predicted by the

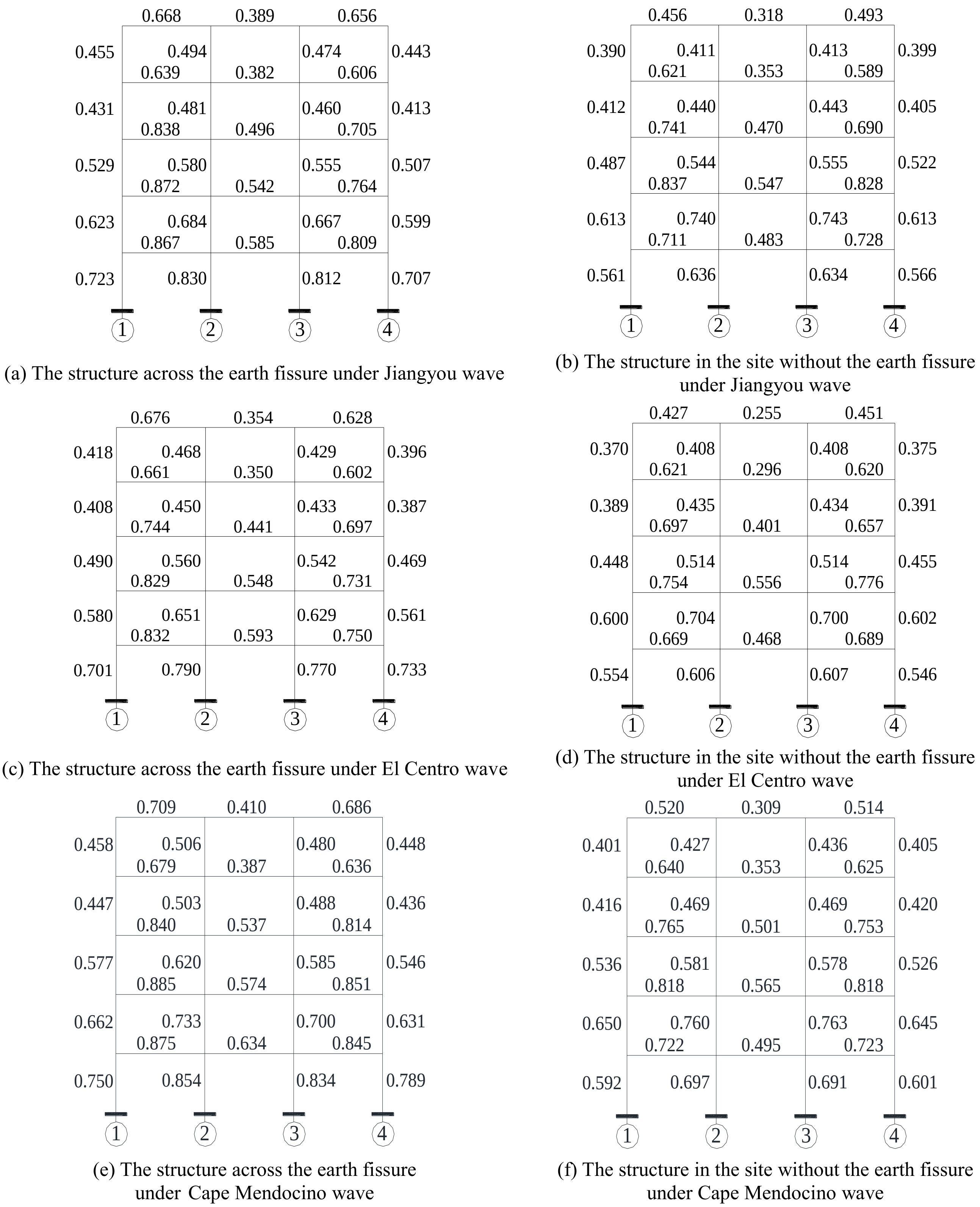

Fig. 12 The seismic damage index on structural members

numerical model were consistent with those obtained from the experiments. The maximum acceleration of each story increased gradually along the height of the structure under each earthquake wave. In addition, the maximum acceleration at each story from the experimental results was a little more than that from numerical results. The deviations between the numerical and experimental results were small and did not affect the variation pattern. Therefore, the finite element model is reasonable to predict the response of the structure across the earth fissure.

Table 6 Damage indices of each story in two cases

Seismic wave	Story	Structure across the earth fissure			Structure without the earth fissure		
		0.1 g	0.2 g	0.4 g	0.1 g	0.2 g	0.4 g
Jiangyou record	5	0.120	0.092	0.132	0.099	0.076	0.107
	4	0.111	0.088	0.122	0.128	0.099	0.123
	3	0.139	0.129	0.147	0.138	0.139	0.149
	2	0.171	0.139	0.163	0.198	0.181	0.201
	1	0.205	0.192	0.218	0.160	0.162	0.162
El-Centro record	5	0.327	0.250	0.331	0.246	0.198	0.256
	4	0.323	0.247	0.323	0.313	0.240	0.340
	3	0.389	0.303	0.370	0.361	0.287	0.359
	2	0.445	0.392	0.435	0.443	0.410	0.463
	1	0.459	0.446	0.491	0.404	0.346	0.419
Cape Mendocino record	5	0.543	0.517	0.556	0.459	0.453	0.476
	4	0.537	0.501	0.550	0.496	0.483	0.516
	3	0.635	0.617	0.672	0.597	0.565	0.632
	2	0.741	0.715	0.793	0.795	0.763	0.818
	1	0.887	0.842	0.908	0.698	0.663	0.755

5. Numerical simulation damage analysis

5.1 Damage analysis on structural members

According to the deformation and plastic energy dissipation of structural members at each story obtained by the numerical simulation, the damage index of each member was calculated based on Chen model. Fig. 12 depicts the damage index of structural members under the seismic waves with the PGA of 0.4 g (strong earthquake).

Damage indices of beams in the middle span were smaller than those in the side span, and the damage indices of interior columns were larger than those exterior columns. The damage indices of the beams were larger than those of the columns in general, which indicates that the damage degrees of beams were more serious than that of the columns under the same seismic wave. This finding was also observed in the testing.

For the structure across the earth fissure, the damage indices of members of beams and columns showed obvious laws of hanging wall and foot wall. The damage indices of structural members located on the hanging wall were larger than those located on the foot wall. Along the direction of story height, the maximum damage indices of the structure were found in the ground story, and damage indices decreased from the ground story to the fourth story. However, the damage indices of members at the fifth story were a little larger than those at the fourth story. The results showed that the structural members experienced the most serious damage at the first story whereas the structural members experienced the minimum damage at the fourth story.

For the structure on the site without earth fissure, there was little difference in damage indices of members along the longitudinal direction. Along the direction of story height, the maximum damage indices of the structure were found in the second story, and damage indices decreased from the second story to both sides. This indicated that the structural members experienced the most serious damage at the second story.

By comparing the two cases, it was found that the damage indices of the members of the structure across the earth fissure were larger than those of the structure on the site without earth fissure at the same location. For the structure across the earth fissure, the damage of structural members was related to the location on the earth fissure site, and the damage of members in the hanging wall was greater than those in the foot wall. The existence of earth fissure would significantly amplify the intensity of the seismic wave propagating to structural foundations. The intensity varied at different positions under the earth fissure site, resulted in a non-uniform seismic excitation for the structure across the earth fissure. Generally, the intensity of the seismic excitation was greater in the hanging wall than that in the foot wall with the same distance from the earth fissure.

5.2 Damage analysis on story-level

Based on Chen model (Chen *et al*. 2010), the damage indices of each story were calculated under seismic waves with the PGA of 0.1 g, 0.2 g and 0.4 g, as shown in Table 6. In the calculation, Eh is the energy dissipation of all the members at a story, which colud be directly obtained in the simulation results.

From Table 6, it can be seen that the damage indices of each story were different under different seismic waves, but the overall change trends were consistent. The damage indices on story-level of the structure across the earth fissure were larger than those of structure without the earth fissure at the same story, indicating the existence of earth fissure would significantly amplify structural seismic response.

For the structure across the earth fissure, the damage indices on the ground story were the largest, indicating the ground story was the weakest story of the structure. The second story was the weakest story of the structure without the earth fissure. This indicated that the weak story of the structure was changed due to the effect of earth fissure.

Table 7 Damage indices of the structure in two cases

Case	Seismic waves	Damage index						
		0.05 g	0.1 g	0.15 g	0.2 g	0.3 g	0.4 g	0.6 g
The site with the earth fissure	Jiangyou wave	0.119	0.172	0.296	0.421	0.537	0.752	0.899
	El Centro wave	0.097	0.154	0.282	0.380	0.483	0.718	0.861
	Cape Mendocino wave	0.131	0.178	0.334	0.429	0.579	0.783	0.959
The site without the earth fissure	Jiangyou wave	0.095	0.163	0.271	0.391	0.492	0.680	0.822
	El Centro wave	0.085	0.156	0.247	0.341	0.450	0.649	0.791
	Cape Mendocino wave	0.117	0.166	0.297	0.406	0.541	0.716	0.893

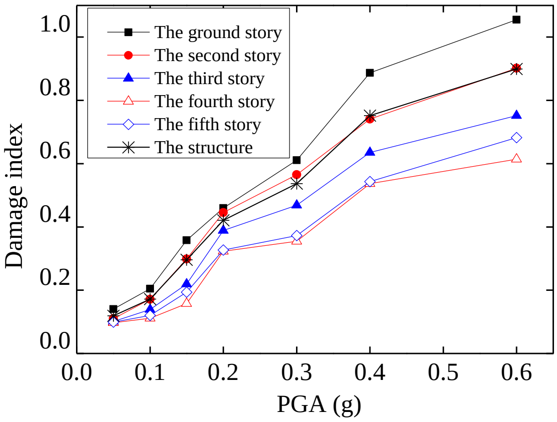

(a) The structure across the earth fissure under Jiangyou wave

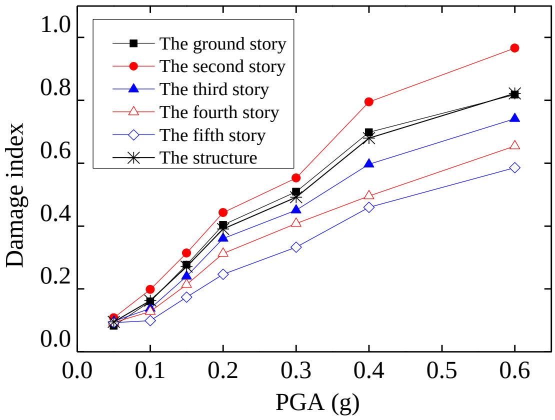

(b) The structure in the site without the earth fissure under Jiangyou wave

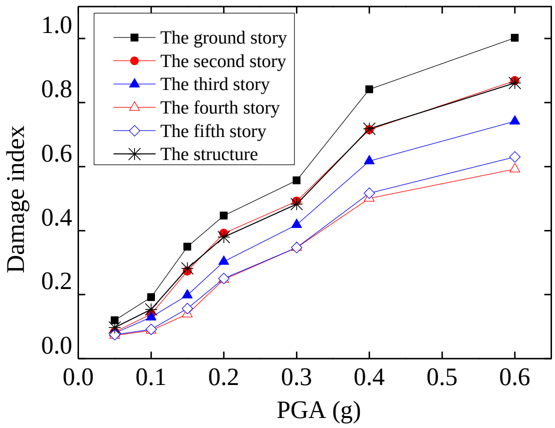

(c) The structure across the earth fissure under El Centro wave

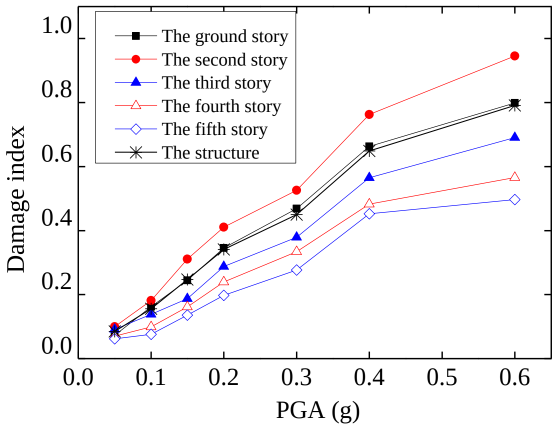

(d) The structure in the site without the earth fissure under El Centro wave

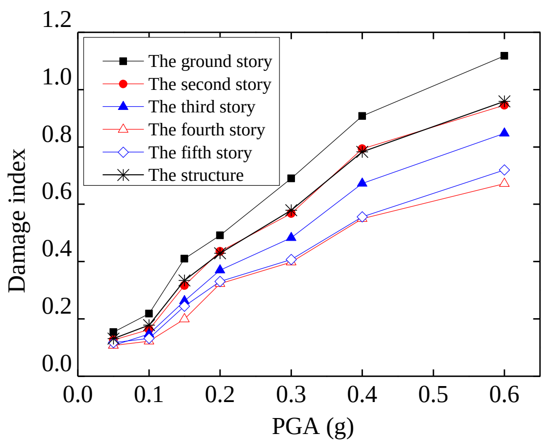

(e) The structure across the earth fissure under Cape Mendocino wave

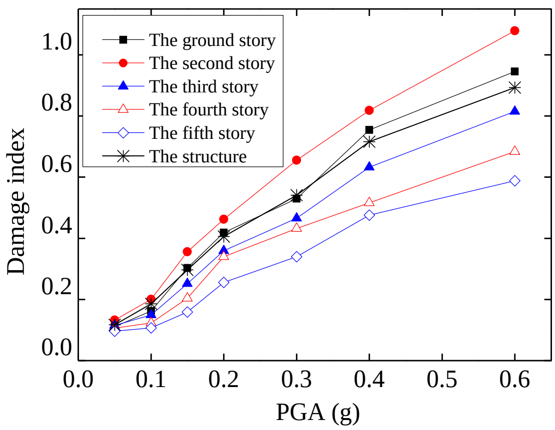

(f) The structure in the site without the earth fissure under Cape Mendocino wave

Fig. 13 The seismic damage index on story-level and structure-level

5.3 Damage analysis on structure-level

Based on the weighted combination method proposed by Ou, the damage indices at structure-level were calculated under different seismic waves, which show in Table 7.

It is noted that the maximum inter-story drift ratios under the Cape Mendocino wave were larger than those under the Jiangyou and El Centro wave, which illustrated that the seismic damage degree of the structure was related to the type of seismic waves.

Under Cape Mendocino wave with the PGA of 0.1 g (small earthquake), the damage indices of the structure in two cases were less than 0.2, indicating that the structure was basically intact. Under Cape Mendocino wave with the PGA of 0.2 g (moderately strong earthquake) and 0.4 g (strong earthquake), the structure in the two types of site was in the state of medium damage and severe damage. However, the damage indices of the structure across the earth fissure were larger than those without the earth fissure. Under Cape Mendocino wave with the PGA of 0.6 g (extremely strong earthquakes), the structure without the earth fissure was still at the state of severe damage whereas the structure across the earth fissure had collapsed. Therefore, the earth fissure would enlarge the damage on structure-level for the structure across it.

Fig. 13 depicts the results of the damage on structure-level and story-level for two cases. Among them, the damage on story-level was calculated by the Method O using Chen model. For the structure across the earth fissure, the weakest story of the structure was the ground story, and the curve of the damage indices on structure-level was very close to the curve of the damage indices of the ground story; for the structure without the earth fissure, the weakest story of the structure is the second story, and the curve of the damage indices on structure-level was very close to the curve of the damage indices of the second story. Therefore, the existence of earth fissure would change the position of the weak story, which controlled the seismic performance of the structure. Compared with the structure without the earth fissure, the seismic performance of the structure across the earth fissure degraded under different seismic waves with the same intensity.

6. Conclusıons

To estimate the damage degree of the RC frame structure across the earth fissure under the earthquake excitation, damage indices of the model structure were calculated based on some common damage models. By comparing the calculation results using different methods with the experimental results, a weighted combination method using Chen model was selected in this paper as the seismic damage evaluation. Then the influence of earth fissure on structural damage was analyzed by numerical simulation. Some conclusions drawn from this study are presented below:

- Based on different damage models, the experimental observation and the damage states corresponding to the damage indices were compared under different seismic waves. The Chen model, together with the method proposed by Ou, constitutes an integrated damage assessment system for the structure across the earth fissure.
- The acceleration response of each story calculated from the finite element model matches well to those of the experimental results.
- For the structure across the earth fissure, the damage of structural members was related to the location in the earth fissure site, and the damage of members in the hanging wall was greater than that in the foot wall. In addition, the damage degrees of members of the structure across the earth fissure were larger than those of the structure without the earth fissure at the same location. Therefore, the existence of earth fissure would change the distribution of structural damage, and enlarge the damage degree of members at the same location.
- The earth fissure would change the position of the weak story, which controlled the seismic performance of the structure. Under the same earthquake intensity, the damage degree of the structure across the earth fissure was greater than that of the structure without the earth fissure.

Acknowledgments

This work has been supported by the National Natural Science Foundation of China (Grant No. 51278395), the Science and Technology Project of Ministry of Housing and Urban-Rural Development of China (No. 2019-K-044) and Natural Science Foundation of Shaanxi Province (No. 2018JZ5008). The authors are grateful for all the all reviewers and editors for their warm work and thoughtful suggestions that have helped improve this paper substantially.

References

Ayalew, L., Yamagishi, H. and Reik, G. (2004), “Ground cracks in Ethiopian Rift Valley: facts and uncertainties”, *Eng. Geology*, **75**(3-4), 309-324. https://doi.org/10.1016/j.enggeo.2004.06.018.

Budhu, M. and Adiyaman, I. (2012), “Earth fissure formation from groundwater pumping and the influence of a stiff upper cemented layer”, *Quart. J. Eng. Geology Hydrogeol.*, **45**(2), 197-205. https://doi.org/10.1144/1470-9236/10-030.

Chen, L.Z., Jang, H.J. and Lu, X.l. (2010), “Modified Park-Ang damage model for reinforced concrete structures”, *J. Tong Ji Univ. (Nat. Sci.)*, **38**(8), 1103-1107.

Dipasquale, E. and Cakmak, A.S. (1987), “Detection and Assessment of Seismic Structural Damage”.

Dong, J., Ma, H., Zhang, N., Liu, Y. and Mao, Z. (2018), “Seismic damage assessment of steel reinforced recycled concrete column-steel beam composite frame joints”, *Earthq. Struct.*, **14**(1), 73-84. https://doi.org/10.12989/eas.2018.14.1.073.

Ghobarah, A., Abou-Elfath, H. and Biddah, A. (2015), “Response-based damage assessment of structures”, *Earthq. Eng. Struct. Dyn.*, **28**(1), 79-104. https://doi.org/10.1002/(SICI)1096-9845(199901)28:1%3C79::AID-EQE805%3E3.0.CO;2-J.

Ghosh, S. and Collins, K.R. (2010), “Merging energy-based design criteria and reliability-based methods: exploring a new concept”, *Earthq. Eng. Struct. Dyn.*, **35**(13), 1677-1698.

https://doi.org/10.1002/eqe.602.

Jachens, R.C. and Holzer, T.L. (1982), "Differential compaction mechanism for earth fissures near Casa Grande, Arizona", *Geological Soc. Amer. Bull*., **93**(10), 998-1012. https://doi.org/10.1130/00167606(1982)93%3C998:DCMFEF%3E2.0.CO;2.

Kostinakis, K. and Morfidis, K. (2017), "The impact of successive earthquakes on the seismic damage of multistorey 3D R/C buildings", *Earthq. Struct*., **12**(1), 1-12. https://doi.org/10.12989/eas.2017.12.1.001.

Krawinkler, H. and Moncarz, P.D. (1981), "Theory and application of experimental model analysis in earthquake engineering", Nasa Sti/recon Technical Report No. 82.

Kunnath, S.K., Heo, Y.A. and Mohle, J.F. (2009), "Nonlinear uniaxial material model for reinforcing steel bars", *J. Struct. Eng*., **135**(4), 335-343. https://doi.org/10.1061/(ASCE)0733-9445(2009)135:4(335).

Li, C.J., Tang, X.M. and Ma, T.H. (2006), "Land subsidence caused by groundwater exploitation in the Hangzhou-Jiaxing-Huzhou Plain, China", *Hydrogeol. J*., **14**(8), 1652-1665. https://doi.org/10.1007/s10040-006-0092-6.

Li, S., Tian, J.B. and Liu, Y.H. (2017), "Performance-based seismic design of eccentrically braced steel frames using target drift and failure mode", *Earthq. Struct*., **13**(5), 443-454. https://doi.org/10.12989/eas.2017.13.5.443.

Liu, M.M. (2015), "Study on shaking table model test design scheme of mechanical response of ground fissure strongly under seismic load", *Appl. Mech. Mat*., **716**, 456-459. https://doi.org/10.4028/www.scientific.net/AMM.716-717.456.

Liu, N.N., Huang, Q.B., Ma, Y.J., Bulut, R., Peng, J.B., Fan, W. and Men, Y.M. (2017), "Experimental study of a segmented metro tunnel in a ground fissure area", *Soil Dyn. Earthq. Eng*., **100**, 410-416. https://doi.org/10.1016/j.soildyn.2017.06.018.

Niu, D.T. and Ren, L.J. (1996), "A modified seismic damage model with double variables for reinforced concrete structures", *Earthq. Eng. Eng. Dyn*., **16**(4), 44-54.

Ou, J.P., He, Z., Wu, B. and Qiu, F.W. (1999), "Seismic damage performance-based design of reinforced concrete structures", *Earthq. Eng. Eng. Dyn*. **1**, 21-30.

Park, Y.J. and Ang, H.S. (1985), "Mechanistic seismic damage model for reinforced concrete", *J. Struct. Eng*., **111**(4), 722-739. https://doi.org/10.1061/(ASCE)0733-9445(1985)111:4(722).

Peng, J.B. (2012), "Disaster of the ground fissures in Xi'an", Science Press, Beijing.

Peng, J.B., Qiao, J.W., Leng, Y.Q., Wang, F.Y. and Xue, S.Z. (2016), "Distribution and mechanism of the ground fissures in Wei River Basin, the origin of the Silk Road", *Environ. Earth Sci*., **75**(8), 1-12. https://doi.org/10.1007/s12665-016-5527-3.

Rajendran, C.P., Earnest, A., Rajendran, K., Das, R.D. and Kesavan, S. (2003), "The 13 September 2002 North Andaman (Diglipur) earthquake: An analysis in the context of regional seismicity", *Current Sci*., **84**(7), 919-924.

Sancio, R.B., Bray, J.D., Stewart, J.P., Youd, T.L., Durgunoğlu, H.T., Önalp, A., Seed, R.B., Christensen, C., Baturay, M.B. and Karadayılar, T. (2002), "Correlation between ground failure and soil conditions in Adapazari, Turkey", *Soil Dyn. Earthq. Eng*., **22**(9-12), 1093-1102. https://doi.orrg/10.1016/S0267-7261(02)00135-5.

Wang, Z.F., Shen, S.L., Cheng, W.C. and Xu, Y.S. (2016), "Ground fissures in Xi'an and measures to prevent damage to the Metro tunnel system due to geohazards", *Environ. Earth Sci*., **75**(6), 1-11. https://doi.org/10.1007/s12665-015-5169-x.

Wartman, J., Rodriguez-Marek, A., Repetto, P.C., Keefer, D.K., Rondinel, E., Zegarra-Pellane, J. and Baures, D. (2003), "Ground Failure", *Earthq. Spectra*, **19**(S1), 35-56.

Wei Cai Ping, Di, W. and Dong, W.D. (2013), "The geotechnical investigation report of underground civil air defense engineering of TangYan Road", Northwest Research Institute of Engineering Investigations and Design, Xi'an. China.

Wu, B. and Ou, J.P. (1993), "Analysis on response and damage of reinforced concrete structures under mainshock and aftershock", *J. Build. Struct*., **14**(5), 45-53.

Xiong, Z.M., Chen, X., Wang, Y., Zhang, C. and Zhuge, Y. (2019), "Shaking table tests on braced reinforced concrete frame structure across the earth fissure under earthquake", *Struct. Des. Tall Spec. Build*., **28**(1), e1559. https://doi.org/10.1002/tal.1559.

Xiong, Z.M., Chen, X., Zhang, C., Huo, X.P. and Zhuge, Y. (2018), "Shaking table tests of RC frame structure across the earth fissure under earthquake", *Struct. Des. Tall Spec. Build*., **27**(14), e1496. https://doi.org/10.1002/tal.1496.

Xiong, Z.M., Wei, J., Guo, Y.L. and Wang, B. R. (2018), "A study on the dynamic response of structures across ground fissures under non-uniform seismic", *J. Vib. Shock*, **37**(4), 197-202.

Yu, Q.G., Shao, S.J. and Zheng, W.K. (2010), "Geo-engineering disasters in Xi'an ground fracture area and its control measures", *J. Nat. Disasters*, **19**(3), 45-51.

Zhao, W.S., Chen, W.Z., Zheng, P.Q. and Yu, J.X. (2013), "Choice and implementation of seismicwave input method in numerical calculation for underground engineering", *Chinese J. Rock Mech. Eng*., **32**(8), 1579-1587.

CC